J Supercond Nov Magn (2015) 28:1231–1236
DOI 10.1007/s10948-014-2897-1

ORIGINAL PAPER

Electronic Structure and Properties of Superconducting Materials with Simple Fermi Surfaces

T. Jarlborg

Received: 31 July 2014 / Accepted: 5 November 2014 / Published online: 11 December 2014

Abstract The electronic structures of the ground state for several different superconducting materials, such as cuprates, conventional 3-dimensional superconductors, doped semiconductors, and low-dimensional systems, are quite different and sometimes in contrast to what supposed to make a superconductor. Properties like the Fermi-surface (FS) topology, density of states (DOS), stripes, electron-phonon coupling (λ_{ep}), and spin fluctuations (λ_{sf}) are analyzed in order to find clues to what might be important for the mechanism of superconductivity. A high DOS at E_F is important for standard estimates of $\lambda's$, but it is suggested that superconductivity can survive a low DOS if the FS is simple enough. Superconducting fluctuations are plausible from coupling to long-wavelength modes in underdoped cuprates, where short coherence length is a probable obstacle for long-range superconductivity. Thermal disorder is recognized as a limiting factor for large T_C independently of doping.

Keywords Electronic structure · Superconductivity · Thermal disorder · Cuprates

1 Introduction

The electronic structures of transition metals (TM) and their alloys and compounds show that several d-bands cross the Fermi energy E_F. Their Fermi surfaces are complex and occupy about all parts of the Brillouin zone (BZ). Calculations of electron-phonon coupling(EPC) $\lambda_{ep} = NI^2/M\omega^2$, where N is the density of states (DOS) at E_F, M an atomic mass, and ω a weighted phonon frequency, became quite popular in 1970s when the matrix element I could be determined quite easily from the band structure by the rigid muffin-tin approximation (RMTA) [1]. Then, from Bardeen, Cooper, and Schrieffer (BCS) [2] or the McMillan formula [3], the superconducting T_C is estimated, and the results for pure elements, TM alloys, TM nitrides and carbides, C15, and A15 compounds are quite reasonable [4–11]. The calculated T_C is not precise, but good superconductors are clearly separated from less good or bad ones, with the observation that a high T_C needs a high N. The quantitative agreement with observed T_C is improved when the pair-breaking effect from spin fluctuations are taken into account through the coupling constant λ_{sf} [12–15]. But, on the other hand, superconductivity in the very lightly doped semiconductors $SrTiO_3$ (STO), WO_3, diamond (C), and Si [16–22] is not easy to understand. Their DOS are very small and T_C goes to zero already at modest dopings [23–29], despite the fact that the DOS normally should go up with doping. The problems with the high-T_C cuprates are well known [30]. The band gap in undoped cuprates is absent in density functional theory (DFT) band calculations. Moreover, EPC alone is probably too weak to explain T_C, since Ns are small with few bands at E_F and simple FSs. Spin-phonon coupling (SPC) enforces λ's [31, 32], and spin fluctuations could be determining for T_C [33], as also could be the case for low T_C's in ZrZn2 [34] and Fe under high pressure [35–37].

Here, we make an effort to understand the difficult cases by doing some corrections of how EPC is to be evaluated for materials with simple FS.

T. Jarlborg (✉)
DPMC, University of Geneva, 24 Quai Ernest-Ansermet, 1211 Geneva 4, Switzerland
e-mail: Thomas.Jarlborg@unige.ch

2 Results and Discussion

2.1 Bands and Coupling Constants

The band structure results presented here are made using the linear muffin-tin orbital (LMTO) method [39, 40] and the local spin-density approximation (LSDA) [41]. Electronic correlation beyond that contained within DFT is disregarded. It is sometimes argued that correlation is too strong for having traditional bands in undoped cuprates when the d-band is half filled. But DFT bands and FSs for doped cuprates agree well with angular-resolved photoemission spectroscopy (ARPES) and angular correlation of positron annihilation radiation (ACAR) [30, 43, 44]. The calculation of I in the RMTA leads to dipole transitions that couple states ℓ to $\ell \pm 1$. The d-bands in TM compounds are hybridized with p and f, and this fact makes I_{RMTA} large. From its name, it is understood that the potential is displaced "rigidly" to get the dipolar matrix element as a first-order change of the band energy as function of the displacement. However, in ionic systems, there are also changes in the local Madelung potential when an atom is displaced, which leads to a monopolar matrix element [45]. This makes the coupling largest for unhybridized bands, as for the Cu-d band in cuprates, the d-band in doped $SrTiO_3$ (STO) and WO_3, and the p-band in hole-doped C and Si. Since I_q (at k-points on the FS) is the first-order change of the band energy ϵ_k, it can also be obtained from the change in band energy when a phonon modifies the potential. The advantage with this method is that both the monopole and dipole contribution are included. The result also takes screening into account when the calculations are self-consistent. This method has been used in the nearly free electron (NFE) model [46, 47], as well as in fully self-consistent LMTO calculations [32], to show that the largest I_q appears for phonon q-vectors that span the FS. Only few q-vectors generate gaps at E_{F}, and together with the dominant contribution from nested FS, it leads to involvement of rather few q-modes for simple FS [48, 49].

2.2 Doped Semiconductors

The FSs in electron-doped STO and hole-doped C and Si consist of simple small pockets at the Γ-points, so that all of the electron-lattice interactions are concentrated to a small fraction of the BZ near the zone center. The logarithm of the BCS equation for T_{C}, $M\omega_q^2 = N_q I_q^2 \log(1.13\hbar\omega/k_{\mathrm{B}}T_{\mathrm{C}})$, permits a separation of the dominant energy cost from excitations of phonons with vector $q \sim k_{\mathrm{F}}$ from the electronic energy gain from different pieces of the FS at N_q. An average of ω^2 over the entire phonon spectrum includes frequencies up to the Debye frequency for q-vectors at the limit of the BZ, but only up to a much smaller cutoff for weakly doped semiconductors, since no gain in total energy comes from larger q (see Fig. 1). The cost of phonon energy is therefore much reduced, and it compensates for the low N. A simple estimation of these energies for a Debye phonon DOS, $F(\omega)$, and free electron DOS (both in three dimensions) at low doping show also that this energy balance becomes less favorable at higher doping, so that T_{C} goes down [49]. Thus, the absence of large q phonon excitations can explain superconductivity from acoustic small q, low-energy phonons in weakly doped semiconductors despite their low DOS and the drop in T_{C} for increased doping [49]. According to this, only long-wavelength phonons appear at $T = 0$ together with lattice disorder from zero-point motion (ZPM).

2.3 Cuprates

The FS in cuprates involves large q vectors between nested sections of the 2-dimensional circular FS. The FS becomes almost diamond shaped at optimal doping, when the FS reaches the X-point of the BZ and the DOS has a van-Hove singularity peak. This permits a reduced number (ideally only two) of phonon/spin mode excitations between electron states on two parallel FS sheets in order to create a gap over the whole FS. This is not as exactly as the small q situation in doped semiconductors, but the 2-dimensional structure with few flat sections of the FS is likewise favorable to superconductivity despite a low N [49]. In this context, it can be noted that T_{C} in Ba_2CuO_3 is found to be much larger than in La_2CuO_4 [50–52]. The electronic interplane interaction is reduced in the former material because of less apical oxygens, and it makes the FS even more flat at optimal doping than in La_2CuO_4 [49, 53, 54]. Additional ordering of dopants into static stripes has been suggested to lead to a segmentation of the FS and enhanced T_{C} [55–57]. It is not clear if such enhancement can come from fewer phonon/spin excitations or from increased DOS because of stripe order [58]. It can also be noted that weak signs of ferromagnetism are present at high doping [59, 60]. However, the doping is very high and beyond the concentration where superconductivity can be found. Anti-ferromagnetic (AFM) order is installed on Cu at zero doping. The amplitude of AFM moments and local exchange splittings decreases for increasing doping, which introduces a doping dependence of the coupling constant for spin fluctuations (λ_{sf}). Calculations of the strength of λ_{sf} are uncertain because of the problem with LDA to describe the static AFM order and the band gap for undoped cuprates [61], but as expected, there is a clear decrease of λ_{sf} as the function of doping h (holes/Cu) [46]. In addition, phonons and spin waves are mutually enforcing each other through SPC [31, 32].

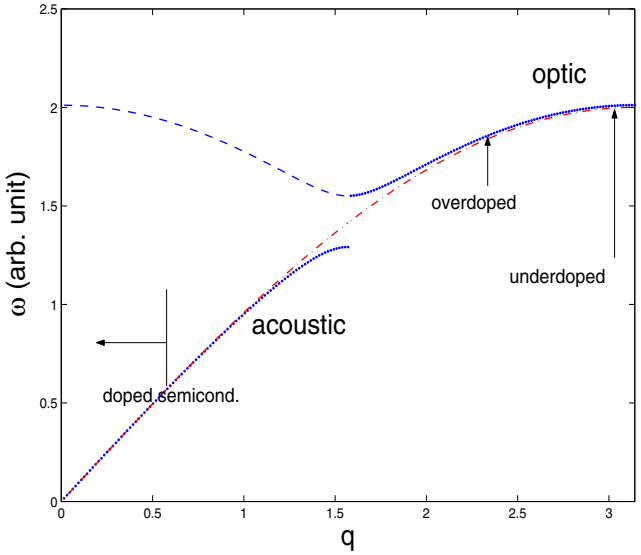

Fig. 1 (*Color online*) Schematic phonon dispersion along k_x. It is argued that the largest EPC in doped semiconductors is found for the acoustic low-energy mode. Optic modes in underdoped cuprates are not efficient for long-range superconductivity, but acoustic modes grow in importance at higher doping

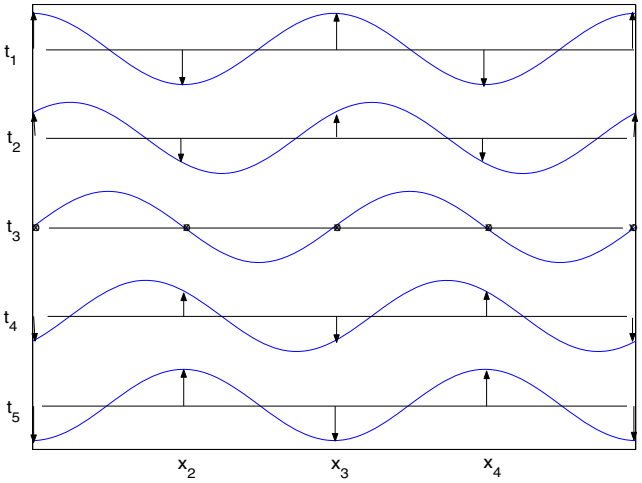

Fig. 2 (*Color online*) Time evolution of a pure optic phonon/spin wave mode for five atoms along x. The *arrows* indicate atomic displacements and/or magnetic moments for each atomic site. Note that all distortions/moments are zero at time t_3

2.4 Disorder and Fluctuations in Cuprates

The AFM spin arrangement on Cu sites along x in undoped cuprates can be described by $V_Q \exp(-iQx)$, where V_Q is the exchange splitting and $Q = \pi/a_0$. Doping makes the gap to appear at lower energy, and the band (ϵ_k) is crossing E_F for $k = Q - q$. The AFM order is modulated by $\exp(iqx)$, and the spin potential becomes

$$V(x) = V_{Q-q} \exp(-i(Q-q)x)) \tag{1}$$

Optimal doping corresponds to $q \approx Q/4$, with "stripes" covering four sites, and the exchange splitting decreases for larger q [32, 46]. The vector q is small at very low doping, and the spin arrangement is almost like an optic wave (see Fig. 2). The spin distribution of an optic wave (or atomic displacements for phonons) is regularly zero over a large region (at times t_3 in Fig. 2), which in principle makes λ time dependent. An acoustic wave, however, has always the same shape (Fig. 3). If q is very small (almost optic), with very wide stripes covering several tens of atoms, then the wave is intact as for a short acoustic wave. But rather wide regions between the stripes have very small spin/distortion amplitudes (for the short wave in Fig. 3, one of four sites has zero spin/distortion). The suggestion is that long-range superconductivity is not possible if the regions with small spin/distortion amplitudes are wider than the coherence length. Alternatively, superconductivity could still be possible, but at a lower T_C than what is expected from the large amplitudes within the stripes. Possible short-range superconducting fluctuations within the stripes are sufficient for a high T_C and can be the cause of the pseudogap at T^*.

Some numbers give substance to this idea: The BCS coherence length, $\xi = 2\hbar v_F/\pi\Delta$, where v_F is the Fermi velocity (taken from the calculated bands in La_2CuO_4 [62] to be between 10 and 35 $\cdot 10^4$ m/s from underdoping (UD) near $h = 0.05$ to optimal doping (OD) near $h = 0.15$) and Δ the superconducting gap (here $2\Delta = 3.5T_C$, and $T_C = T^*$ is supposed to be due to superconducting fluctuations. Typical T^* is in the range of 60–30 meV from UD to OD [43]) from which ξ can be estimated to be between $1a_0$ and $7a_0$ at low T, respectively. This gives very approximately $\xi \sim 30h$ (units of a_0). The wavelengths, Λ, of spin waves and phonons are related to doping, h holes/Cu. From LMTO supercell calculations, $\Lambda = 2/h$ in units of a_0 (Λ is the length of a unit cell along [100] in which one spin wave or two phonon waves can fit) and the amplitudes $V_{(Q-q)}$ are calculated to be of the order 25-17 mRy between UD and OD [32]. In the wave drawn in Fig. 3, the zero spin/displacement region covers one eighth of the cell. By assuming that ξ must be larger than the width x_c in which $V(x)$ is smaller than ~ 0.25 of the maximal $V_{(Q-q)}$, we get the condition $x_c < \arcsin(0.25)/\pi/h$, which gives x_c smaller than 1.6 to 0.5 a_0 from UD to OD. Thus, $\xi > x_c$ for h smaller than about 0.07, for which there should be no long-range superconductivity according to this reasoning.

The value of ξ increases when T gets closer to T_C, but at a higher temperature, there are thermal disorders of the lattice [63]. The latter is known to induce band broadening ($\Delta\epsilon_k$) and temperature-dependent variations of non-superconducting properties in many materials [64–68]. There will be irregular variations of the local potential as a

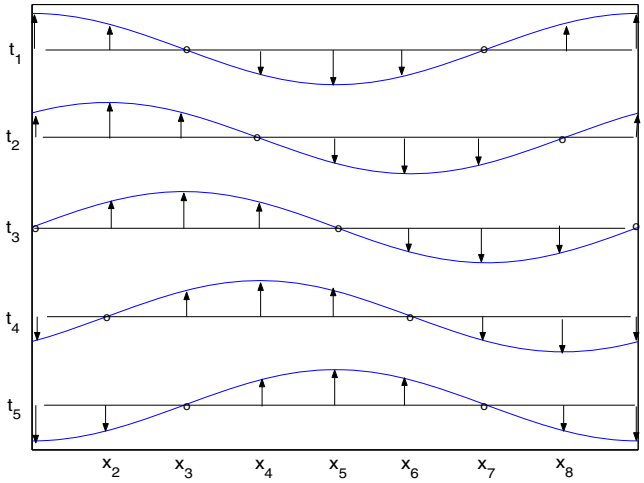

Fig. 3 (*Color online*) Time evolution of an acoustic phonon for nine atoms along x. The *arrows* indicate atomic displacements. Note that the wave is identical at all times except for the phase. A cuprate spin wave would have AFM spin orientation on near neighbors, as in Fig. 2, but all modulated by the long-range envelope function

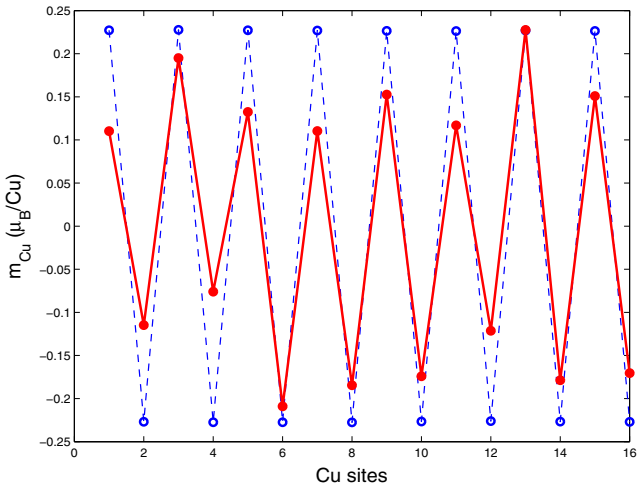

Fig. 4 (*Color online*) Magnetic moments per atom on Cu in ordered (*blue open circles connected by broken lines*) and disordered (*red circles connected by lines*) $La_{32}Cu_{16}O_{64}$, where an applied field of ± 8 mRy sets up an AFM spin alignment along the 100 direction in the supercell. The disorder corresponds to that of room temperature

function of time, more so at a high temperature and for a soft lattice. Well-defined waves along the lattice are required in order to generate a neat gap at E_F, when the Coulomb part and/or the spin part of the potential is close to cosine-like shape, as in Eq. 1. Thermal disorder generates random potential fluctuations on the atomic sites, and if the fluctuation amplitudes, V_T, are comparable to $V_{(Q-q)}$, then they will interfere with the cosine wave and finally make it unrecognizable. Cuprates are unique because of the AFM order on Cu, and the spin-polarized part of V_T turns out to be more sensitive to disorder than the Coulomb part. Disorder makes large shifts of the local Madelung potential, but the exchange splitting (χ_{Cu}) on different Cu sites develops quite differently, and the calculation show that V_T at room temperature (RT) for a disordered supercell of $La_{32}Cu_{16}O_{64}$ is larger than $V_{(Q-q)}$ calculated for a cosine SPC wave in a Hg-based cuprate [61]. Calculations of $V_{(Q-q)}$ for simple AFM in undoped $La_{32}Cu_{16}O_{64}$ show that the average of moments and $V_{(Q-q)}$ goes down with disorder. At RT, the averages are approximately two thirds of those for the ordered structure, and the amplitude of individual moments varies by a factor of three (or more for weak spin waves), which shows that AFM waves are much perturbed by disorder (see Fig. 4). The average valence electron charge on Cu increases from 10.39 to 10.47 at this level of disorder, as if the disorder reduced the level of hole doping. Band broadening is proportional to the rms-average of V_T, and long-range superconductivity could be suppressed by thermal disorder if V_T exceeds the superconducting energy gap. The band broadening from thermal disorder is difficult to calculate, since it needs large supercells. In other materials, the averaged broadening $\Delta\epsilon$ is calculated to be of the order of 50 meV at RT when the average of the atomic displacements is about 0.1 Å [64, 67]. Here, for undoped LCO, $\Delta\epsilon_k$ is about 28 meV in the Coulomb part and about 60 meV when the calculations are made for an AFM configuration. Potential shifts on Cu caused by disorder are typically larger than $\Delta\epsilon$ on about one fourth of all Cu.

The coupling strength $V_{(Q-q)}$ for spin fluctuations increases when $h \to 0$, because the AFM state is more and more developed at low doping and finally the cuprates become insulators with stable AFM moments at zero doping. But T_C is known to have a maximum for $h \approx 0.15$. In a very approximate drawing of a phase diagram in Fig. 5, we suggest that superconducting fluctuations can survive at low doping up to large temperature proportional to $V_{(Q-q)}$. No fluctuations appear above T_C at high doping, because $V_{(Q-q)}$ is not large. Thermal disorders suppress superconductivity at all dopings.

If disorder puts a limit to the long-range superconductivity, one may search for ways to recuperate a higher T_C by some kind of stabilization of superconducting fluctuations. At low T, it seems that longer ξ can be obtained via higher v_F, as probably is achieved naturally in many cuprates by a static pseudogap. This would permit an extended pairing at UD, but superconductivity will be weaker because a higher v_F implies a lower $N(E_F)$ and weaker coupling. Anharmonicity could also be favorable, since the thickness of a zone with low $V_{(Q-q)}$ will be narrower for a step-like wave than for a cosine wave. At higher T, it is difficult to get rid of thermal disorder. Higher coupling constants, especially for spin fluctuations, should be efficient to enforce clean spin waves, but the problem is that also V_T will profit from high exchange enhancement. Therefore, bad influence from

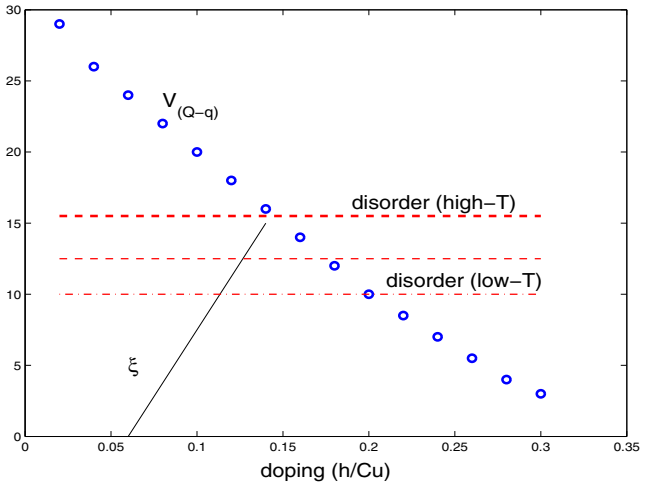

Fig. 5 (*Color online*) A sketch of a phase diagram for cuprates. The *blue circles* indicate the coupling strength $V_{(Q-q)}$, but T_C is zero to the left of the line for ξ due to a short coherence length. Thermal disorder will gradually destroy well-defined waves at a certain level indicated by the *red horizontal lines*. Long-range superconductivity would be possible below the lines, but only fluctuations on the left side of the ξ-line

disorder could spoil the effect of enforced spin waves. Structural disorder will be smaller in a stiffer lattice at a given T, and since the spin disorder is largely an effect of the structural disorder, it suggests that lattice hardening would help. This can be achieved by applying pressure, but the strength of the spin wave ($V_{(Q-q)}$) must not decrease when the volume is reduced. The idea that a higher $N(E_F)$ provides a larger gain in electronic energy from a superconducting gap, and hence stronger coupling constants and higher T_C, is still valid at large disorder. How to modify the cuprate band structures in order to get higher DOS without destroying other properties might be difficult; perhaps, ordering of impurities into stripes is a promising way [55].

3 Conclusion

Electron-phonon interaction and coupling from spin fluctuations are largest when the q vector of the lattice/spin wave is equal to the k-vector on the FS, at least for the cases of simple FSs of cuprates and some doped semiconductors. This is evident for NFE bands, but it is also seen in the ab initio calculated band structures of cuprates [32]. For a simple FS, it is therefore possible that superconductivity relies only on a few phonon/spin excitations, which makes superconductivity possible even if $N(E_F)$ is small. In contrast, for a complicated FS, practically the entire phonon/spin spectrum is needed to open gaps over all parts of the FS. Further, it can be noted that a pure optic mode should have a frequency-dependent coupling. A long-wavelength modulation of an optic mode, as for underdoped cuprates, behaves as a normal acoustic mode, but wide regions with small coupling could prevent long-range superconductivity. Shorter wavelengths of acoustic modes at higher doping do not have this property, but thermal disorder at high temperature will cause potential fluctuations which compete with and prevent long-range superconductivity. Based on such mechanisms, we speculate that the disorder prevents long-range superconductivity, but that superconducting fluctuations are left behind and they will cause a pseudogap below T^*. There are no obvious solutions for an easy transformation of superconducting fluctuation into long-range superconductivity with higher T_C, but the sensitivity of T_C due to varied conditions is expected to be different at low and high doping.

References

1. Gaspari, G.D., Gyorffy, B.L. Phys. Rev. Lett. **28**, 801 (1972)
2. Bardeen, J., Cooper, L.N., Schrieffer, J.R. Phys. Rev. **108**, 1175 (1957)
3. McMillan, W.L. Phys. Rev. **167**, 331 (1968)
4. Papaconstantopoulos, D.A., Boyer, L.L., Klein, B.M., Williams, A.R., Moruzzi, V.L., Janak, J.F. Phys. Rev. **B15**, 4221 (1977)
5. Pictet, O., Jarlborg, T., Peter, M. J. Phys. **F17**, 221 (1987)
6. Dacorogna, M., Jarlborg, T., Junod, A., Pelizzone, M., Peter, M. J. Low Temp. Phys. **57**, 629 (1984)
7. Jarlborg, T., Freeman, A.J. Phys. Rev. **22**, 2332 (1980)
8. Klein, B.M., Boyer, L.L., Papaconstantopoulos, D.A. Phys. Rev. Lett. **42**, 530 (1979)
9. Arbman, G., Jarlborg, T.: Solid State Commun. **26**, 857 (1978)
10. Jarlborg, T., Junod, A., Peter, M.: Phys. Rev. **B27**, 1558 (1983)
11. Jarlborg, T., Manuel, A.A., Peter, M. Phys. Rev. **B27**, 4210 (1983)
12. Berk, N.F., Schrieffer, J.R.: Phys. Rev. Lett. **17**, 433 (1966)
13. Fay, D., Appel, J.: Phys. Rev. **B22**, 3173 (1980)
14. Jarlborg, T.: Solid State Commun. **57**, 683 (1986)
15. Daams, J.M., Mitrovič, B., Carbotte, J.P.: Phys. Rev. Lett. **46**, 65 (1981)
16. Ekimov, E.A., Sidorov, V.A., Bauer, E.D., Mel'nik, N.N., Curro, N.J., Thompson, J.D., Stishov, S.M.: Nature **428**, 542 (2004)
17. Bustarret, E., Marcenat, C., Achatz, P., Kačmarčik, J., Lévy, F., Huxley, A., Ortega, L., Bourgeois, E., Blaise, X., Débarre, D., Boulmer, J.: Nature **444**, 465 (2006)
18. Raub, C.J., Sweedler, A.R., Jensen, M.A., Broadston, S., Matthias, B.T.: Phys. Rev. Lett. **13**, 752 (1964)
19. Shooley, J.F., Hosler, W.R., Cohen, M.L.: Phys. Rev. Lett. **12**, 474 (1964)
20. Koonce, C.S., Cohen, M.L., Shooley, J.F., Hosler, W.R., Pfeiffer, E.R.: Phys. Rev. **163**, 380 (1965)
21. Suzuki, H., Bando, H., Ootuka, Y., Inoue, I.H., Yamamoto, T., Takahashi, K., Nishihara, Y.: J. Phys. Soc. Jpn. **65**, 1529 (1996)
22. Lin, X., Zhu, Z., Fauqué, B., Behnia, K.: Phys. Rev. **X3**, 021002 (2013)
23. Mattheiss, L.F.: Phys. Rev. **B6**, 4718 (1972)
24. Jarlborg, T.: Rev, Phys. **B61**, 9887 (2000)
25. Jarlborg, T.: Journal of Magn. Magn. Mater. **267**, 261 (2003)
26. Boeri, L., Kortus, J., Andersen, O.K.: Phys. Rev. Lett. **93**, 237002 (2004)

27. Lee, K.W., Pickett, W.E.: Phys. Rev. Lett. **93**, 237003 (2004)
28. Blase, X., Adessi, C., Connétable, D.: Phys. Rev. Lett. **93**, 237004 (2004)
29. Xiang, H.J., Li, Z., Yang, J., Hou, J.G., Zhu, Q.: Phys. Rev. **B70**, 212504 (2004)
30. Pickett, W.E.: Rev. Mod. Phys. **61**, 433 (1989)
31. Jarlborg, T.: Rev. Phys. **B64**, 060507(R) (2001)
32. Jarlborg, T.: Physica **C454**, 5 (2007)
33. Monthoux, P., Pines, D., Lonzarich, G.: Nature **450**, 1177 (2007)
34. Santi, G., Dugdale, S.B., Jarlborg, T.: Phys. Rev. Lett. **87**, 247004 (2001)
35. Shimizu, K., Kimura, T., Furomoto, S., Takeda, K., Kontani, K., Onuki, Y., Amaya, K.: Nature (London) **412**, 316 (2001)
36. Jaccard, D., Holmes, A., Behr, G., Onuki, Y.: Phys. Lett. **A299**, 282 (2002)
37. Jarlborg, T.: Physica **C385**, 513 (2003)
38. Jarlborg, T.: Lett. Phys. **A300**, 518 (2002)
39. Andersen, O.K.: Phys. Rev. **B12**, 3060 (1975)
40. Barbiellini, B., Dugdale, S.B., Jarlborg, T. Comput. Mater. Sci. **28**, 287 (2003)
41. Kohn, W., Sham, L.J.: Phys. Rev. **140**, A1133 (1965)
42. Gunnarsson, O., Lundquist, B.I.: Phys. Rev. B. **13**, 4274 (1976)
43. A. Damascelli, Z.-X. Shen, Z. Hussain: Rev. Mod. Phys. **75**, 473 (2003). and references therein
44. Barbiellini, B., Genoud, P., Henry, J.Y., Hoffmann, L., Jarlborg, T., Manuel, A.A., Massidda, S., Peter, M., Sadowski, W., Scheel, H.J., Shukla, A., Singh, A.K., Walker, E.: Phys. Rev. B **43**, 7810 (1991)
45. Jarlborg, T.: Solid State Commun. **67**, 297 (1988)
46. Jarlborg, T.: Rev, Phys. **B76**, 140504(R) (2007)
47. Jarlborg, T.: Rev, Phys. **B79**, 094530 (2009)
48. Jarlborg, T.: Solid State Commun. **151**, 639 (2011)
49. Jarlborg, T.: Solid State Commun. **181**, 15 (2014)
50. Liu, Q.Q., Yang, H., Qin, X.M., Yu, Y., Yang, L.X., Li, F.Y., Yu, R.C., Jin, C.Q.: Phys. Rev. **B74**, 100506 (2006)
51. Gao, W.B., Liu, Q.Q., Yang, L.X., Yu, Y., Li, F.Y., Jin, C.Q., Uchida, S.: Phys. Rev. **B80**, 094523 (2009)
52. Geballe, T.H., Marezio, M.: Physica C **469**, 680 (2009)
53. Jarlborg, T., Barbiellini, B., Markiewicz, R.S., Bansil, A.: Phys. Rev. B **86**, 235111 (2012). doi:10.1103/PhysRevB.86.235111
54. Jarlborg, T., Bianconi, A., Barbiellini, B., Markiewicz, R.S., Bansil, A., Supercond, J.: Nov. Magn. (2013). doi:10.1007/s10948-013-2142-3
55. Jarlborg, T., Bianconi, A.: Phys. Rev. B **87**, 054514 (2013). doi:10.1103/PhysRevB.87.054514
56. Poccia, N., Fratini, M., Ricci, A., Campi, G., Barba, L., Vittorini-Orgeas, A., Bianconi, G., Aeppli, A., Bian coni, A.: Nat. Mater. **10**, 733 (2011)
57. Chmaissem, O., Grigoraviciute, I., Yamauchi, H., Karppinen, M., Marezio, M.: Phys. Rev. B **82**, 104570 (2010)
58. Jarlborg, T.: Phys, Appl. Lett. **94**, 212503 (2009)
59. Barbiellini, B., Jarlborg, T.: Phys. Rev. Lett. **101**, 157002 (2008). doi:10.1103/PhysRevLett.101.157002
60. Sonier, J.E., Kaiser, C.V., Pacradouni, V., Sabok-Sayr, S.A., Cochrane, C., MacLaughlin, D.E., Komiya, S., Hussey, N.E.: PNAS **107**, 17313 (2010). doi:10.1073/pnas.1007
61. Jarlborg, T. Phys, J. Condens. Matter **16**, L173 (2004)
62. Jarlborg, T.: Rev, Phys. **B84**, 064506 (2011)
63. Jarlborg, T., Santi, G.: Physica C **329**, 243 (2000)
64. Jarlborg, T.: Phys. Rev. **B59**, 15002 (1999)
65. Pedrazzini, P., Wilhelm, H., Jaccard, D., Jarlborg, T., Schmidt, M., Hanfland, M., Akselrud, L., Yuan, H.Q., Schwarz, U., Grin, Yu., Steglich, F.: Phys. Rev. Lett. **98**, 047204 (2007)
66. Delaire, O., Marty, K., Stone, M.B., Kent, P.R., Lucas, M.S., Abernathy, D.L., Mandrus, D., Sales, B.C.: PNAS **108**, 4725 (2011)
67. Jarlborg, T., Chudzinski, P., Giamarchi, T.: Phys. Rev. B **85**, 235108 (2012)
68. Jarlborg, T.: Rev. Phys. **B89**, 184426 (2014)